PHYSICAL REVIEW B **93**, 060505(R) (2016)

Coupling to real and virtual phonons in tunneling spectroscopy of superconductors

Jasmin Jandke,[1] Patrik Hlobil,[2] Michael Schackert,[1] Wulf Wulfhekel,[1] and Jörg Schmalian[2,3]
[1]*Physikalisches Institut, Karlsruher Institut für Technologie, 76131 Karlsruhe, Germany*
[2]*Institut für Theorie der Kondensierten Materie, Karlsruher Institut für Technologie, 76131 Karlsruhe, Germany*
[3]*Institut für Festkörperphysik, Karlsruher Institut für Technologie, 76344 Karlsruhe, Germany*
(Received 10 April 2015; revised manuscript received 23 December 2015; published 4 February 2016)

Fine structures in the tunneling spectra of superconductors have been widely used to identify fingerprints of the interaction responsible for Cooper pairing. Here, we show that for scanning tunneling microscopy (STM) of Pb, the inclusion of inelastic tunneling processes is essential for the proper interpretation of these fine structures. For STM the usual McMillan inversion algorithm of tunneling spectra must therefore be modified to include inelastic tunneling events, an insight that is crucial for the identification of the pairing glue in conventional and unconventional superconductors alike.

DOI: 10.1103/PhysRevB.93.060505

I. INTRODUCTION

Conventional superconductivity is caused by the attractive interaction between electrons near the Fermi energy mediated by phonons [1]. This leads to the formation of a gap 2Δ in the single particle density of states (DOS) of the electrons, and to quasiparticle peaks above and below the gap [2,3]. Eliashberg extended the BCS theory to the limit of larger dimensionless electron-phonon coupling constants λ, including a realistic electron-phonon coupling and a detailed structure of the phonon spectrum [4]. As a consequence, the quasiparticle peaks near the Fermi surface are modified due to the interaction with phonons, leading to fine structures in the electronic DOS near the peaks of the Eliashberg function $\alpha^2F(\omega)$ shifted by Δ. $\alpha^2F(\omega)$ is the phonon DOS $F(\omega)$, weighted by the energy dependent electron-phonon coupling strength $\alpha^2(\omega)$. These fine structures are due to the excitation of virtual phonons (see Fig. 1). Experimentally, these fine structures in the electronic DOS have been detected with electron tunneling spectroscopy on planar junctions [5–11]. In the pioneering work of McMillan and Rowell [12], the Eliashberg function could be reconstructed from the superconducting DOS by an inversion algorithm, taking into account the interaction of electrons and virtual phonons. This method has been used to identify fingerprints of the phononic pairing glue in the electronic spectrum and thus to determine the pairing mechanism leading to superconductivity [13,14]. It counts as a hallmark of condensed matter physics.

An alternative way to determine the Eliashberg function is to measure the energy dependence of the scattering of electrons with real phonons in the normal state using inelastic tunneling spectroscopy (ITS) [15–18] (see Fig. 1). This method is more direct, as the second derivative of the tunneling current I with respect to the bias voltage U is, under rather general assumptions, directly proportional to $\alpha^2F(\omega)$ [19]. Recently, this method has been combined with scanning tunneling microscopy (STM) to obtain local information on the Eliashberg function of Pb on a Cu(111) substrate [20].

In this paper, we determine experimentally and analyze theoretically the tunneling conductance of Pb that is affected by the coupling to real phonons via inelastic tunneling and virtual phonons via many-body renormalizations. Comparing the two approaches to determine $\alpha^2F(\omega)$ on the same sample with the same tip of a low-temperature STM, we show that interpreting the tunneling spectra of superconductors via the McMillan inversion algorithm (and thus solely by its elastic contribution) can be an incomplete description. We demonstrate that inelastic contributions to the tunneling current can, in general, be of the same order as the elastic contribution. We show that we can understand experimental STM data from Pb tunneling in the normal and superconducting state, taking into account both elastic and inelastic tunneling processes. The combined analysis of elastic and inelastic tunneling processes is important to correctly identify fingerprints of the relevant interactions in the electronic DOS and to identify the pairing glue for superconductivity. This is essential for conventional superconductors, such as Pb, but is expected to be even more important for unconventional pairing states, where an electronic pairing interaction is expected to fundamentally change its character upon entering the superconducting state.

II. EVIDENCE OF INELASTIC STM FROM NORMAL STATE DATA

We start with experimental data for STM measurements on lead. Measurements were performed with a home-build Joule-Thomson low-temperature STM (JT-STM) [21] at temperatures about 0.8 K. The JT-STM contains a magnet which allows one to suppress superconductivity. In order to ensure that there is no significant inelastic signal of the tip at $|U| < 15$ mV, we use a chemically etched tungsten tip,

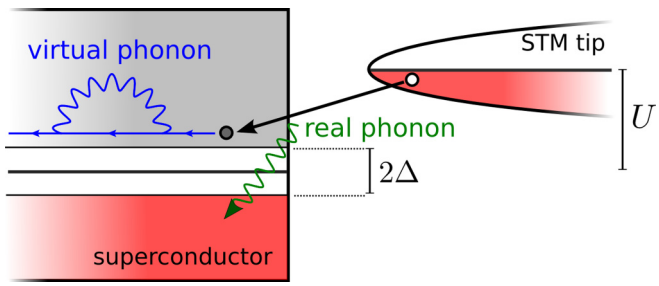

FIG. 1. Illustration of the inelastic tunneling processes from a sharp tip (right) into a superconductor (left) in real space. Filled states are shown in red color with energy along the vertical axis. The inelastic tunneling process is accompanied by the excitation of real phonons (green).

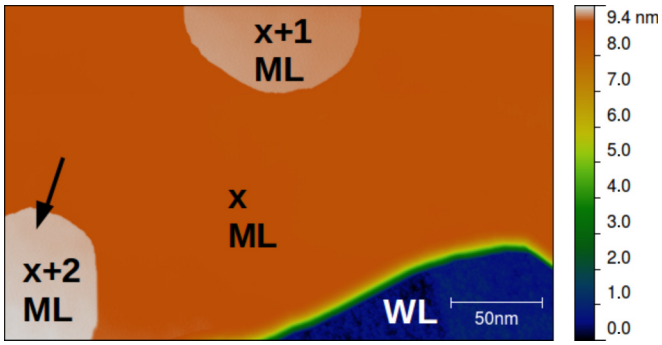

FIG. 2. STM topography of Pb on Si(111) (300×175 nm^2, 1 V, 1 nA). The thickness of the island was determined to $x \approx 30$ monolayers.

known to have a weak electron-phonon coupling [22]. The highly n-doped Si(111) crystals were carefully degassed at 700 °C for several hours and then flashed to 1150 °C for 30 s to remove the native oxide. Lead was evaporated at room temperature from a Knudsen cell with a nominal thickness of 19 monolayers (ML). After deposition, the samples were immediately transferred to the cryogenic STM. In agreement with previous studies [23–25], flattop, wedgelike islands of local thickness around 30 ML were observed (see Fig. 2), i.e., extended three-dimensional (3D) islands appear on top of a metallic wetting layer (WL).[1] The islands are Pb single crystals with their ⟨111⟩ axis perpendicular to the substrate [24,26,27]. The first (second) derivative of the tunneling current dI/dU (d^2I/dU^2) of the islands was measured using a lock-in amplifier with a modulation voltage of $U_{\rm mod} = 439$ μV.

While the electrons in the ≈30 ML Pb film on Si have quantized k_z, leading to the flat island growth, the phonon DOS of the finite thickness films is rather similar to that of bulk Pb, as indicated by first principles calculations [28,29]. As a first measurement, we therefore determine $\alpha^2F_{\rm tun}(\omega)$ of lead directly with ITS in the normal state. Pb islands were forced to the normal state by applying a magnetic field of 1 T normal to the sample plane. Since the sample is in the normal state, no renormalization of the BCS density of states

[1]Note that the extensions of the lead islands are typically larger than the 400×400 nm^2 STM images of the surfaces giving a minimal island size of 0.16 μm^2. This excludes Coulomb blockade as source for the spectral features discussed later.

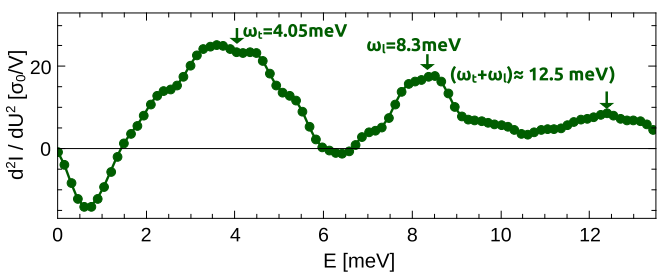

FIG. 3. Second derivative $d^2I/dU^2 \sim \alpha^2F_{\rm tun}(eU)$ measured in the normal conducting state ($T = 0.8$ K, $B = 1$ T).

near the Fermi energy due to virtual phonons arises. Thus renormalization effects by virtual phonons can be neglected in d^2I/dU^2 and experimental features in d^2I/dU^2 correspond to inelastic tunneling. Figure 3 shows the measured d^2I/dU^2 spectrum clearly revealing the two characteristic phonon peaks that are also seen in the Eliashberg function $\alpha^2F(\omega)$ determined by Ref. [12]. Below, we show explicitly that in the normal state d^2I/dU^2 is proportional to $\alpha^2F_{\rm tun}(eU)$. These peaks at $U = 4.05$ mV $\approx \omega_t$ and $U \approx 8.3$ mV $\approx \omega_l$ (FWHM $\gamma_t = 1.076$ meV and $\gamma_l = 0.60$ meV) coincide with the energies of the van Hove singularities of the transversal and longitudinal the phonons of lead [29,30]. The additional peak at $U \approx 12.5$ mV can be explained by tunneling processes via two-phonon emission.[2]

The key implication from Fig. 3 for the superconducting state is, however, that we must include inelastic contributions to the superconducting tunneling spectrum in a consistent fashion. Before we present our experimental data of the superconducting state, we summarize the theoretical description of the tunneling conductance in the superconducting state including inelastic contributions.

III. TRANSFER HAMILTONIAN FOR ELASTIC AND INELASTIC STM WITH PHONONS

The Hamiltonian $\mathcal{H} = \mathcal{H}_0 + \mathcal{H}_{\rm t}$ used in our analysis of the combined substrate and tip consists of free electrons in the tip and electrons interacting with phonons in the substrate (we set $\hbar = 1$):

$$\mathcal{H}_0 = \sum_{\boldsymbol{p},\sigma} \epsilon^T_{\boldsymbol{p}} c^\dagger_{\boldsymbol{p},\sigma} c_{\boldsymbol{p},\sigma} + \sum_{\boldsymbol{k},\sigma} \epsilon^S_{\boldsymbol{k}} c^\dagger_{\boldsymbol{k},\sigma} c_{\boldsymbol{k},\sigma} + \sum_{\boldsymbol{q},\mu} \omega_{\boldsymbol{q},\mu} a^\dagger_{\boldsymbol{q},\mu} a_{\boldsymbol{q},\mu} + \frac{1}{\sqrt{V_S}} \sum_{\substack{\boldsymbol{k},\boldsymbol{k}' \\ \sigma,\mu}} \alpha_{\boldsymbol{k}-\boldsymbol{k}',\mu} c^\dagger_{\boldsymbol{k},\sigma} c_{\boldsymbol{k}',\sigma} \phi_{\boldsymbol{k}-\boldsymbol{k}',\mu}. \quad (1)$$

Here, $\phi_{\boldsymbol{q},\mu} = a_{\boldsymbol{q},\mu} + a^\dagger_{-\boldsymbol{q},\mu}$ is proportional to the lattice displacement, where $a_{\boldsymbol{q},\mu}$ is the the phonon annihilation operator for momentum $\boldsymbol{q}$ and phonon branch μ and with dispersion $\omega_{\boldsymbol{q},\mu}$. $c^\dagger_{\boldsymbol{k}/\boldsymbol{p},\sigma}$ are the electron annihilation operators for the two subsystems: the tip (quasimomentum $\boldsymbol{p}$, dispersion $\epsilon^T_{\boldsymbol{p}}$, and volume V_T) and the superconductor (quasimomentum $\boldsymbol{k}$, dispersion $\epsilon^S_{\boldsymbol{k}}$, and volume V_S). For the latter we include the electron-phonon coupling $\alpha_{\boldsymbol{k}-\boldsymbol{k}',\mu}$ that gives rise to superconductivity. The electron-phonon interaction in the tip is assumed to be small. In addition, the tunneling part of the Hamiltonian includes elastic and inelastic tunneling processes [19,31]:

$$\mathcal{H}_{\rm t} = \frac{1}{\sqrt{V_T V_S}} \sum_{\substack{\boldsymbol{k},\boldsymbol{p} \\ \sigma}} T_{\boldsymbol{k},\boldsymbol{p}} c^\dagger_{\boldsymbol{k},\sigma} c_{\boldsymbol{p},\sigma} + \text{H.c.},$$

$$T_{\boldsymbol{k},\boldsymbol{p}} = T^{\rm e}_{\boldsymbol{k},\boldsymbol{p}} + \frac{1}{\sqrt{V_S}} \sum_{\boldsymbol{q},\mu} T^{\rm i}_{\boldsymbol{k},\boldsymbol{p},\boldsymbol{q},\mu} \alpha_{\boldsymbol{q},\mu} \phi_{\boldsymbol{q},\mu} + O\left(\phi^2_{\boldsymbol{q},\mu}\right). \quad (2)$$

The first term of the tunneling amplitude $T_{\boldsymbol{k},\boldsymbol{p}}$ describes the elastic tunneling part, and the second term corresponds to

[2]Note that also the second peak may already include such two-phonon processes.

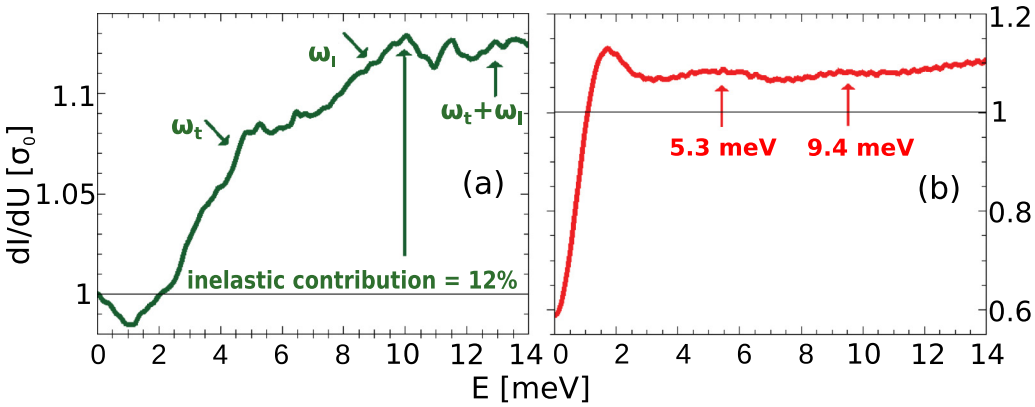

FIG. 4. Differential conductance dI/dU in the normal (a) and superconducting (b) state measured on the island marked by the arrow in Fig. 2. The curves are normalized to the zero bias conductance $\sigma(0)$ in the normal state.

electron transitions via the emission/absorption of phonons (see Fig. 1). It is proportional to the bulk electron-phonon coupling $\alpha_{\boldsymbol{q},\mu}$ [19]. There can also be processes with a higher number of phonons, which will be discussed later.

In order to determine the tunneling current, we assume that the DOS of the tip is constant $\nu_T(\omega) \approx \nu_T^0$ and that the tunneling amplitudes are independent of momenta and phonon branches $T^{\mathrm{e}}_{\boldsymbol{k},\boldsymbol{p}} = t^{\mathrm{e}}$ and $T^{\mathrm{i}}_{\boldsymbol{k},\boldsymbol{p},\boldsymbol{q},\mu} = t^{\mathrm{i}}$, which is a reasonable approximation for STM [32]. Then, to leading order in t^{e}, the differential conductance gives the well known result [33–35]

$$\sigma^{\mathrm{e}}(U) = \frac{dI^{\mathrm{e}}}{dU} = -e\sigma_0 \int_{-\infty}^{\infty} d\omega\, n_F'(\omega + eU)\tilde{\nu}_S(\omega). \qquad (3)$$

In the limit that T is smaller than the electronic energy scales, the conductance is just proportional to the normalized electron DOS $\tilde{\nu}_S(\omega) = \nu_S(\omega)/\nu_S^0$, where ν_S^0 is the normal state DOS of the superconductor at the Fermi level. The conductance constant is given by $\sigma_0 = 4\pi e^2 |t^{\mathrm{e}}|^2 \nu_T^0 \nu_S^0$ and n_F is the Fermi function. In the normal state, $\tilde{\nu}_S(\omega)$ is essentially constant for small applied voltages and the second derivative of the elastic current vanishes, as discussed above. In the superconducting state, the opening of the superconducting gap and the excitation of virtual phonons lead to the mentioned fingerprints of superconductivity and the pairing glue in the elastic tunneling spectrum. Below, we determine these structures from the solution of the nonlinear Eliashberg equations for given $\alpha^2F(\omega)$ and compare with our STM experiments.

The inelastic contribution to the differential conductance $\sigma^{\mathrm{i}}(U) = \frac{dI^{\mathrm{i}}}{dU}$ due to the excitation of a single real phonon is, for $U > 0$, given by the convolution

$$\sigma^{\mathrm{i}}(U) = \sigma_0 \frac{|t^{\mathrm{i}}|^2}{|t^{\mathrm{e}}|^2 \nu_S^0} \int_{-\infty}^{\infty} d\omega\, \alpha^2 F^T_{\mathrm{tun}}(eU + \omega)\tilde{\nu}_S(\omega) n_F(\omega), \qquad (4)$$

in the limit that the thermal phonons can be neglected, $T \ll \omega_D$. The function $\alpha^2 F^T_{\mathrm{tun}}(x) = -\int_{-\infty}^{\infty} dy\, \alpha^2 F_{\mathrm{tun}}(y) n_F'(y - x)$ is a thermally broadened version of the weighted phonon DOS $\alpha^2 F_{\mathrm{tun}}(\omega) = \frac{\nu_S^0}{V_S} \sum_{\boldsymbol{q},\mu} |\alpha_{\boldsymbol{q},\mu}|^2 \delta(\omega - \omega_{\boldsymbol{q},\mu})$ that is closely related to the Eliashberg function $\alpha^2F(\omega) = \frac{1}{\nu_S^0 V_S^2} \sum_{\boldsymbol{k},\boldsymbol{k}',\mu} |\alpha_{\boldsymbol{k}-\boldsymbol{k}',\mu}|^2 \delta(\omega - \omega_{\boldsymbol{k}-\boldsymbol{k}',\mu}) \delta(\epsilon^S_{\boldsymbol{k}}) \delta(\epsilon^S_{\boldsymbol{k}'})$. Both have similar features but can differ in fine structure and amplitude.

The result (4) is the generalization of the current in the normal state, where $\frac{d^2I^{\mathrm{i}}}{dU^2}|_{\mathrm{NC}} \sim \mathrm{sgn}(U)\alpha^2 F_{\mathrm{tun}}(e|U|)$ is proportional to the weighted DOS of the phonons (or other collective excitations of the system) (see Refs. [19,31,36,37]). It naturally explains the results of Fig. 3 or the recent STM measurements on Pb [20]. Our measurement further allows for an estimate of the inelastic tunneling amplitude $t^{\mathrm{i}} \approx t^{\mathrm{e}}/D$, which is inversely proportional to the characteristic energy scale of the off-shell electrons involved in the tunneling process. The normal state elastic conductance $\sigma^{\mathrm{e}}(U) \approx \sigma_0$ is not energy dependent for the applied biases U, and we emphasize that all spectra within this paper are normalized to $\sigma_0 = \sigma(0) = \sigma^{\mathrm{e}}(0)$ to point out the existence of inelastic tunneling contributions. The change in the conductance from 0 to 10 mV seen in Fig. 4(a) is purely due to the inelastic tunneling. This leads to the condition $\sigma^{\mathrm{i}}(10\ \mathrm{mV}) \approx 12\%\sigma_0$, where $\sigma(0) = \sigma_0$ is the purely elastic contribution at zero bias. Using the widely accepted Eliashberg function $\alpha^2F(\omega)$ and the experimental DOS for lead [38], we can estimate for the characteristic off-shell electronic energy to be $D \approx 240$ meV. Below, we will see that elastic and inelastic contributions to the fine structure turn out to be comparable in magnitude.

In the superconducting state, the inelastic contribution Eq. (4) has its major contribution slightly below the energy of the phonon peaks shifted by the gap Δ. Since inelastic tunneling opens additional channels to the conductance, it will lead to positive contributions to d^2I/dU^2 at positive bias. Elastic contributions are of opposite sign [see (3)]. Thus, pronounced peaks in the second derivative of the tunneling current due to real phonons are followed by dips of the same amplitude due to virtual phonons (for details, see the discussion of a single phonon mode in the Supplemental Material [39]). As we will see below, we find exactly these features in the tunneling current for the STM experiment on lead.

Tunneling processes with a higher number of excited phonons will give similar terms as in (4) with higher convolutions of the Eliashberg function, such as $\alpha^4 F^2_{\mathrm{tun}}(\omega) = \int d\omega' \alpha^2 F_{\mathrm{tun}}(\omega - \omega')\alpha^2 F_{\mathrm{tun}}(\omega')$, and one can formally absorb this contribution in a redefinition of $\alpha^2 F_{\mathrm{tun}}$ (see the Supplemental Material).

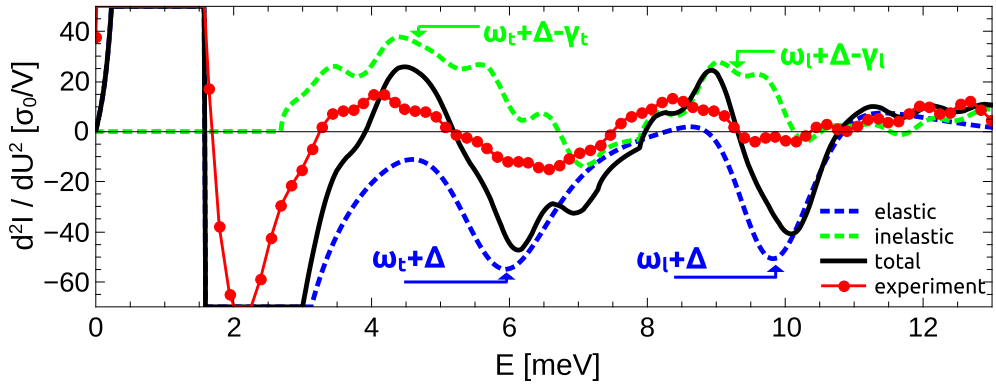

FIG. 5. Comparison of experimental data (red) and theoretical prediction in the superconducting state: Calculated elastic (blue), inelastic (green), and total (black) contributions to d^2I/dU^2 (the elastic current is convoluted with a Gaussian function with a standard deviation $\sigma = 0.31$ meV simulating the experimental broadening due to the modulation voltage of the lock-in technique). Characteristic peak-dip features around the zero axis can only be explained taking into account elastic and inelastic channels ($I^{\text{tot}} = I^{\text{el}} + I^{\text{inel}}$).

IV. COMPARISON OF THEORY AND EXPERIMENTAL DATA IN THE SUPERCONDUCTING STATE

Without magnetic field, the islands are in the superconducting state. As the local thickness of the islands (30 ML $\approx$ 10 nm) is significantly smaller than the bulk coherence length of lead (83 nm [40]), the superconducting gap is not fully developed [23,24,41–45], which implies that the spectral weight of the coherence peaks is accordingly smaller [see Fig. 4(b)]. Besides the Bogoliubov quasiparticle peak, one clearly observes fine structures in the spectrum of the conductance around $U \approx 5.3$ mV and $U \approx 9.4$ mV. These energies correspond to the van Hove singularities in the phonon DOS $F(\omega)$ of lead shifted by the gap $\Delta \approx 1.2$ meV, clearly indicating electron-phonon interaction induced effects. Furthermore, the typical $\omega/\sqrt{\omega^2 - \Delta^2}$ behavior in the BCS DOS is altered by the emergence of inelastic contributions at biases $V_0 > 5$ mV. This is in contrast to previous measurements on planar tunneling junctions of lead [5–10], where these inelastic contributions were about one order of magnitude smaller [16] than in our present experiment. The reason is that inelastic tunneling events are enhanced in STM geometries, if compared to planar tunneling junctions, because the momentum conservation for momenta parallel to the surface is less restrictive [32].

Let us now investigate the second derivative of the tunneling current in the superconducting state, which is significantly more sensitive to the fine structure induced by the electron-phonon interaction. For the theoretical spectrum, we first use a parametrization of the $\alpha^2F(\omega), \mu^*$ from McMillan and Rowell [12,46] to solve the Eliashberg equations numerically [47] to obtain the lead DOS $\nu_S(\omega)$ in the superconducting state. The elastic contribution to the second derivative is then easily calculated using Eq. (3). For the inelastic contribution we use the $\alpha^2F_{\text{tun}}(\omega)$ function (without the negative dip at small voltages $U < 2$ mV that comes from a zero bias anomaly) and the calculated DOS $\nu_S(\omega)$ to determine the convolution in Eq. (4), where the usage of the measured $\alpha^2F_{\text{tun}}(\omega)$ function automatically includes two-phonon processes and yields the correct amplitude for the inelastic tunneling current. Note that the rapid fluctuations on top of the calculated inelastic curve are due to noise of the input data of the calculations, i.e., the experimental inelastic spectrum in the normal state. This noise is caused by residual mechanical vibrations on the level of 300 fm. When convoluting the noisy experimental spectra with the DOS for the calculation of the inelastic contribution in the superconducting state, certain frequencies of the noise are amplified and show up as small fluctuations. Finally, we convoluted the elastic part[3] with a Gaussian distribution (standard deviation $\sigma = 310$ μeV corresponding to an energy resolution of 744 μeV), describing the experimental broadening due to the modulation voltage of the lock-in detection [18].

In Fig. 5 we compare the experimental data with the theoretical prediction of the elastic, inelastic, and total contributions of the second derivative of the current. The experimental data show peak-dip features around the zero axis at positions that correspond to the characteristic longitudinal and transversal phonon energies $\omega_{t/l}$ shifted by the gap $\Delta \approx 1.2$ meV. For both features there is a positive peak at $\approx\omega_{t,l} + \Delta - \gamma_{t,l}$ of the same magnitude as the corresponding dip at $\omega_{t,l} + \Delta$, where $\gamma_{t,l}$ are the half widths of the phonon peaks observed in Fig. 3. This is in contrast to the theoretical elastic $d^2I^{\text{e}}/dU^2 \sim \nu'(-eU)$ curve, which only shows the typical dips around $\Delta + \omega_{t/l}$ predicted by the Eliashberg theory. We note that conventional Eliashberg theory can also have positive peaks, but the following dip will always be significantly more pronounced (see also Fig. 4 in the Supplemental Material). Therefore, the observed peak-dip features cannot be explained by pure elastic tunneling. However, the measured spectrum both in the normal *and* in the superconducting state can naturally be explained when we combine inelastic and elastic contributions. As can be seen, the total theoretical conductance d^2I^{tot}/dU^2 consisting of elastic and inelastic channels fits the experimental peak-dip features much better at the correct energies.

[3]Note that we should not broaden the inelastic contribution as we use the $\alpha^2F_{\text{tun}}(\omega)$ from the normal conductor measurement that already includes broadening—see the Supplemental Material for details.

V. CONCLUSION

In summary, we demonstrated experimentally and theoretically that in normal conducting Pb islands it is possible to directly measure the collective bosonic excitation spectrum, here phonons, using STM. In the normal conducting state, the obtained d^2I/dU^2 spectra are proportional to the weighted phonon DOS $\alpha^2F_{\mathrm{tun}}(\omega)$ and higher convolutions thereof. This is different in the superconducting state of Pb. Here, the obtained second derivative $d^2I/dU^2 = d^2I^{\mathrm{e}}/dU^2 + d^2I^{\mathrm{i}}/dU^2$ spectra are a composition of elastic and inelastic tunneling processes with fine structures in the same energy regime. While the elastic part shows phonon features coming from self-energy corrections (exchange of virtual phonons) that appear mainly as dips in the second derivative of the tunneling current, the inelastic part shows features of $\alpha^2F_{\mathrm{tun}}(\omega)$ shifted by the superconducting gap Δ giving rise to additional peak features of the same amplitude at lower energies (excitation of real phonons). A rather unique signature of these inelastic contributions are peak-dip features in d^2I/dU^2 around zero at $\Delta + \omega_{\mathrm{ph}}$ in the superconducting state. Those cannot be explained by only taking into account the elastic part d^2I^{e}/dU^2. For this reason, the neglect of inelastic processes in STM experiments in general is not justified. Hence, when analyzing STM tunneling spectra via the McMillan inversion algorithm [12,46], which gives the purely elastic contribution, one should carefully subtract the inelastic contributions from the experimental tunneling current. Otherwise, grossly incorrect conclusions about the pairing glue would be deduced from the tunneling spectrum.

Having found out experimentally and theoretically how elastic and inelastic tunneling can be disentangled for STM in conventional superconductors, the approach can be generalized to the investigation of corresponding bosonic structures in high-temperature superconductors, such as cuprates and iron pnictides, in the future. A crucial difference with the phononic pairing glue is that in the case of electronic pairing, the bosonic spectrum undergoes a dramatic reorganization below T_c in the form of a sharp resonance in the dynamic spin excitation spectrum [48–53]. Our results imply that great care must be taken in the proper interpretation of the tunneling spectra of these systems, and that real and virtual bosonic excitations must be disentangled in a fashion similar to our analysis for lead.

ACKNOWLEDGMENTS

The authors acknowledge funding by the DFG under the grant SCHM 1031/7-1 and WU 349/12-1.

[1] J. Bardeen, L. N. Cooper, and J. R. Schrieffer, Phys. Rev. **108**, 1175 (1957).
[2] I. Giaever, Phys. Rev. Lett. **5**, 147 (1960).
[3] J. Nicol, S. Shapiro, and P. H. Smith, Phys. Rev. Lett. **5**, 461 (1960).
[4] G. Eliashberg, Sov. Phys. **11**, 696 (1960).
[5] I. Giaever, H. R. Hart, and K. Mergele, Phys. Rev. **126**, 941 (1962).
[6] J. R. Schrieffer, D. J. Scalapino, and J. W. Wilkins, Phys. Rev. Lett. **10**, 336 (1963).
[7] J. M. Rowell, A. G. Chynoweth, and J. C. Phillips, Phys. Rev. Lett. **9**, 59 (1962).
[8] J. M. Rowell, P. W. Anderson, and D. E. Thomas, Phys. Rev. Lett. **10**, 334 (1963).
[9] W. McMillan and J. Rowell, in *Superconductivity*, edited by R. D. Parks (Dekker, New York, 1969), Vol. 1, pp. 561–611.
[10] I. Giaever, Science **183**, 1253 (1974).
[11] H. Suderow, E. Bascones, A. Izquierdo, F. Guinea, and S. Vieira, Phys. Rev. B **65**, 100519(R) (2002).
[12] W. L. McMillan and J. M. Rowell, Phys. Rev. Lett. **14**, 108 (1965).
[13] D. J. Scalapino and J. W. Wilins, Phys. Rev. **148**, 263 (1966).
[14] J. P. Carbotte, Rev. Mod. Phys. **62**, 1027 (1990).
[15] A. Leger and J. Klein, Phys. Lett. A **28**, 751 (1969).
[16] J. M. Rowell, W. L. McMillan, and W. Feldmann, Phys. Rev. **180**, 658 (1969).
[17] W. Wattamanuik, H. Kreuzer, and J. Adler, Phys. Lett. A **37**, 7 (1971).
[18] J. Klein, A. Léger, M. Belin, D. Défourneau, and M. J. L. Sangster, Phys. Rev. B **7**, 2336 (1973).
[19] M. E. Taylor, Ultramicroscopy **42**, 215 (1992).
[20] M. Schackert, T. Märkl, J. Jandke, M. Holzer, S. Ostanin, E. K. U. Gross, A. Ernst, and W. Wulfhekel, Phys. Rev. Lett. **114**, 047002 (2015).
[21] L. Zhang, T. Miyamachi, T. Tomanić, R. Dehm, and W. Wulfhekel, Rev. Sci. Instrum. **82**, 103702 (2011).
[22] W. McMillan, Phys. Rev. **167**, 331 (1968).
[23] C. Brun, I.-Po. Hong, F. Patthey, I. Yu. Sklyadneva, and R. Heid, P. M. Echenique, K. P. Bohnen, E. V. Chulkov, and W.-D. Schneider, Phys. Rev. Lett. **102**, 207002 (2009).
[24] D. Eom, S. Qin, M.-Y. Chou, and C. K. Shih, Phys. Rev. Lett. **96**, 027005 (2006).
[25] I. B. Altfeder, K. A. Matveev, and D. M. Chen, Phys. Rev. Lett. **78**, 2815 (1997).
[26] H. H. Weitering, D. R. Heslinga, and T. Hibma, Phys. Rev. B **45**, 5991 (1992).
[27] M. Jalochowski, H. Knoppe, G. Lilienkamp, and E. Bauer, Phys. Rev. B **46**, 4693 (1992).
[28] I. Yu. Sklyadneva, R. Heid, K.-P. Bohnen, P. M. Echenique, and E. V. Chulkov, Phys. Rev. B **87**, 085440 (2013).
[29] R. Heid, K.-P. Bohnen, I. Yu. Sklyadneva, and E. V. Chulkov, Phys. Rev. B **81**, 174527 (2010).
[30] B. N. Brockhouse, T. Arase, G. Caglioti, K. R. Rao, and A. D. B. Woods, Phys. Rev. **128**, 1099 (1962).
[31] A. J. Bennett, C. B. Duke, and S. D. Silverstein, Phys. Rev. **176**, 969 (1968).
[32] C. Berthod and T. Giamarchi, Phys. Rev. B **84**, 155414 (2011).
[33] J. Bardeen, Phys. Rev. Lett. **6**, 57 (1961).
[34] M. H. Cohen, L. M. Falicov, and J. C. Phillips, Phys. Rev. Lett. **8**, 316 (1962).
[35] G. D. Mahan, *Many-Particle Physics*, 3rd ed. (Springer, Berlin, 2000).
[36] J. R. Kirtley and D. J. Scalapino, Phys. Rev. Lett. **65**, 798 (1990).
[37] M.-w. Xiao and Z.-z. Li, Physica C: Superconductivity **221**, 136 (1994).
[38] A. V. Gold, Philos. Mag. **5**, 70 (1960).
[39] See Supplemental Material at http://link.aps.org/supplemental/10.1103/PhysRevB.93.060505 for the expressions for the elastic

and in-elastic currents are derived starting from a transfer Hamiltonian approach. The impact of inelastic tunneling for strong-coupling superconductors is outlined using the model of a single phonon mode. Also a brief discussion about the role of experimental broadening is added, as well as the role of multi-phonon processes.

[40] C. Kittel, *Introduction to Solid State Physics* (Wiley, New York, 2005).

[41] T. Nishio, M. Ono, T. Eguchi, H. Sakata, and Y. Hasegawa, Appl. Phys. Lett. **88**, 113115 (2006).

[42] T. Nishio, T. An, A. Nomura, K. Miyachi, T. Eguchi, H. Sakata, S. Lin, N. Hayashi, N. Nakai, M. Machida, and Y. Hasegawa, Phys. Rev. Lett. **101**, 167001 (2008).

[43] S. Qin, J. Kim, Q. Niu, and C.-K. Shin, Science **324**, 1314 (2009).

[44] A. M. Garcia-Garcia, J. D. Urbina, K. Richter, E. A. Yuzbashyan, and B. L. Altshuler, Phys. Rev. B **83**, 014510 (2011).

[45] S. Bose, A. M. García-García, M. M. Ugeda, J. D. Urbina. C. H. Michaelis, I. Brihuega, and K. Kern, Nat. Mater. **9**, 550 (2010).

[46] A. A. Galkin, A. I. D'yachenko, and V. M. Svistunov, Sov. Phys. **39**, 1115 (1974).

[47] J. Schmalian, M. Langer, S. Grabowski, and K. H. Bennemann, Comput. Phys. Commun. **93**, 141 (1996).

[48] J. Rossat-Mignod, L. Regnault, C. Vettier, P. Bourges, P. Burlet, J. Bossy, J. Henry, and G. Lapertot, Physica C **185-189**, 86 (1991).

[49] H. A. Mook, M. Yethiraj, G. Aeppli, T. E. Mason, and T. Armstrong, Phys. Rev. Lett. **70**, 3490 (1993).

[50] H. Fong, P. Bourges, Y. Sidis, L. Regnault, A. Ivanov, G. Gu, N. Koshizuka, and B. Keimer, Nature (London) **398**, 588 (1999).

[51] A. D. Christianson, E. A. Goremychkin, R. Osborn, S. Rosenkranz, M. D. Lumsden, C. D. Malliakas, I. S. Todorov, H. Claus, D. Y. Chung, M. G. Kanatzidis, R. I. Bewley, and T. Guidi, Nature (London) **456**, 930 (2008).

[52] D. S. Inosov, P. B. J. T. Park, D. L. Sun, Y. Sidis, A. Schneidewind, K. Hradil, D. Haug, C. T. Lin, B. Keimer, and V. Hinkov, Nat. Phys. **6**, 178 (2010).

[53] A. Abanov, A. Chubukov, and J. Schmalian, J. Electron Spectrosc. Relat. Phenom. **117**, 129 (2001).